



Design, synthesis and evaluation of novel indirubin-based *N*-hydroxybenzamides, *N*-hydroxypropenamides and *N*-hydroxyheptanamides as histone deacetylase inhibitors and antitumor agents



Duong Tien Anh^a, Pham-The Hai^a, Do Thi Mai Dung^a, Phan Thi Phuong Dung^a,
Le-Thi-Thu Huong^a, Eun Jae Park^b, Hye Won Jun^b, Jong Soon Kang^c, Joo-Hee Kwon^c,
Truong Thanh Tung^{d,e}, Sang-Bae Han^{b,*}, Nguyen-Hai Nam^{a,*}

^a Hanoi University of Pharmacy, 13-15 Le Thanh Tong, Hanoi, Viet Nam

^b College of Pharmacy, Chungbuk National University, 194-31, Osongsangmyung-1, Heungdeok, Cheongju, Chungbuk 28160, Republic of Korea

^c Laboratory Animal Resource Center, Korea Research Institute of Bioscience and Biotechnology, Cheongju, Chungbuk, Republic of Korea

^d Faculty of Pharmacy, PHENIKAA University, Hanoi 12116, Viet Nam

^e PHENIKAA Institute for Advanced Study (PIAS), PHENIKAA University, Hanoi 12116, Viet Nam

ARTICLE INFO

Keywords:

Histone deacetylase (HDAC) inhibitors
N-hydroxybenzamide
 Hydroxamic acids
N-hydroxypropenamide
 Docking simulation
 ADMET profiling

ABSTRACT

Several novel indirubin-based *N*-hydroxybenzamides, *N*-hydroxypropenamides and *N*-hydroxyheptanamides (**4a-h**, **7a-h**, **10a-h**) were designed using a fragment-based approach with structural features extracted from several previously reported HDAC inhibitors, such as SAHA (vorinostat), MGCD0103 (mocetinostat), nexturastat A and PXD-101 (belinostat). The biological results reveal that our compounds showed excellent cytotoxicity toward three common human cancer cell lines (SW620, PC-3 and NCI-H23) with IC₅₀ values ranging from 0.09 to 0.007 μM. The cytotoxicity of the compounds was equipotent or even up to 10-times more potent than adriamycin and up to 205-times more potent than SAHA. Among the series of *N*-hydroxypropenamides, compounds **10a-d** were the most potent HDAC inhibitors as well as cytotoxicity toward the cell lines tested. In addition, the strong inhibitory activities toward HDAC of our compounds were observed with IC₅₀ values of below-micromolar range. Especially, compound **4a** inhibited HDAC6 with an IC₅₀ value of 29-fold lower than that against HDAC2 isoform. Representative compounds **4a** and **7a** were found to significantly arrest SW620 cells at G0/G1 phase. Compounds **7a** and **10a** were found to strongly induce apoptosis in SW620 cells. Docking studies revealed some important features affecting the selectivity against HDAC6 isoform. The results clearly demonstrate the potential of the indirubin-hydroxamic acid hybrids and these compounds should be very promising for further development.

Histone deacetylases (EC 3.5.1.98, HDAC) are the family of enzymes which play a crucial role in removal of the acetyl groups from the lysine termini of histone proteins.¹ To date, 18 HDAC isoforms have been described in human and based on their homology to yeast HDACs, these isoforms are divided into four main classes. Class I with four members (HDACs 1-3, 8), class II with six members (HDACs 4-7, 9, 10) and class IV with only one member (HDAC 11) are characterized as zinc-dependent enzymes, while class III (known as sirtuins 1-7) are NAD⁺-dependent enzyme.² Because of their very critical role in tumor cell biology, HDACs have become one of the most important targets for anticancer drug design and development currently.³ Medicinal chemists worldwide in the past decade have spent extensive research efforts

which resulted in hundreds of structurally diverse and potent HDAC inhibitors. These include principally hydroxamic acids (e.g. suberoylanilide hydroxamic acid, SAHA, Zolinza®), cyclic peptides (e.g. depsipeptide), short-chain fatty acids (e.g. valproic acid), and benzamides.⁴⁻⁹

Hitherto, five HDAC inhibitors have been approved for use clinically to treat several types of cancer. These include suberoylanilide hydroxamic acid (SAHA, Zolinza®), romidepsin (Istodax®), belinostat (PXD101), panobinostat (LBH-589 Farydak®) (approved by the U.S. FDAC in 2006, 2009, 2014, and 2015, respectively), and chidamide (Epidaza®) (approved in 2015 by the Chinese FDA). Dozens of other HDAC inhibitors, such as entinostat (MS-27-527), mocetinostat

* Corresponding authors.

E-mail addresses: shan@chungbuk.ac.kr (S.-B. Han), namnh@hup.edu.vn (N.-H. Nam).

<https://doi.org/10.1016/j.bmcl.2020.127537>

Received 6 July 2020; Received in revised form 8 August 2020; Accepted 2 September 2020

Available online 08 September 2020

0960-894X/© 2020 Elsevier Ltd. All rights reserved.

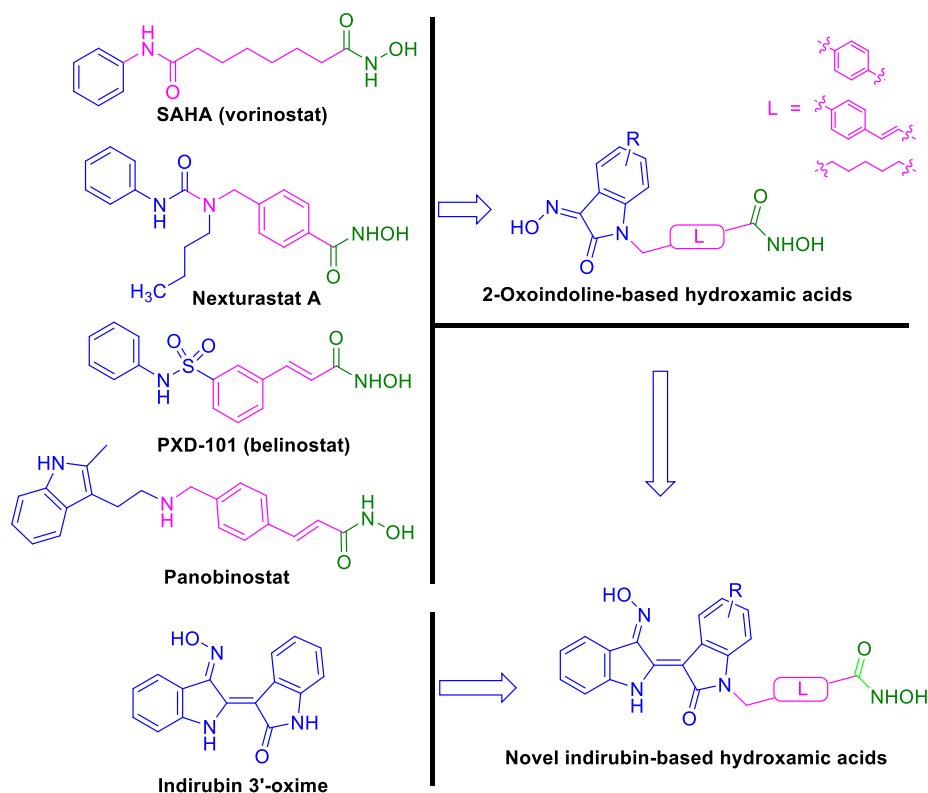


Fig. 1. Rational design of indirubin-based *N*-hydroxybenzamides/*N*-hydroxypropenamides and *N*-hydroxyheptanamides as HDAC inhibitors.

(MGCD0103), and givinostat (ITF2357) are also currently undergoing different phases of clinical trials for several types of cancer.^{10–14}

Previously, we have reported several series of heterocycle-containing hydroxamic acids and *N*-hydroxypropenamides as analogues of SAHA or belinostat/panobinostat,^{15–19} which incorporated different heterocyclic systems, especially 2-oxoindoline one (Fig. 1). In addition, based on the structure of nexturastat A and panobinostat, we also synthesized and evaluated some series of 2-oxoindoline-based *N*-hydroxybenzamides/*N*-hydroxypropenamides (Fig. 1).^{20–22} As a result, the above analogues displayed very potent HDAC inhibitory activities and cytotoxicity against several human cancer cell lines.^{20,22} Furthermore, in the *in vivo* screening in nude mice bearing PC-3 cancer cells, the excellent antitumor activities were observed.^{17,23} In this report, we extended our investigation into novel series of *N*-hydroxybenzamides, *N*-hydroxypropenamides and *N*-hydroxyheptanamides incorporating 2-oxoindoline system (novel 2-oxoindolin-based hydroxamic acids) (Fig. 1). In designing these compounds, we have adopted a hybridization approach, in which 2-oxoindoline moiety has been expanded to include structural features of indirubins (Fig. 1). The indirubins, as represented by indirubin 3'-oxime, are known as anticancer agents.²⁴ It was expected that the indirubins, acting as cap groups, would create more favorable interactions with the amino acid chain at the CAP binding region of HDAC active binding site, thus increasing the affinity of the compounds towards HDACs.

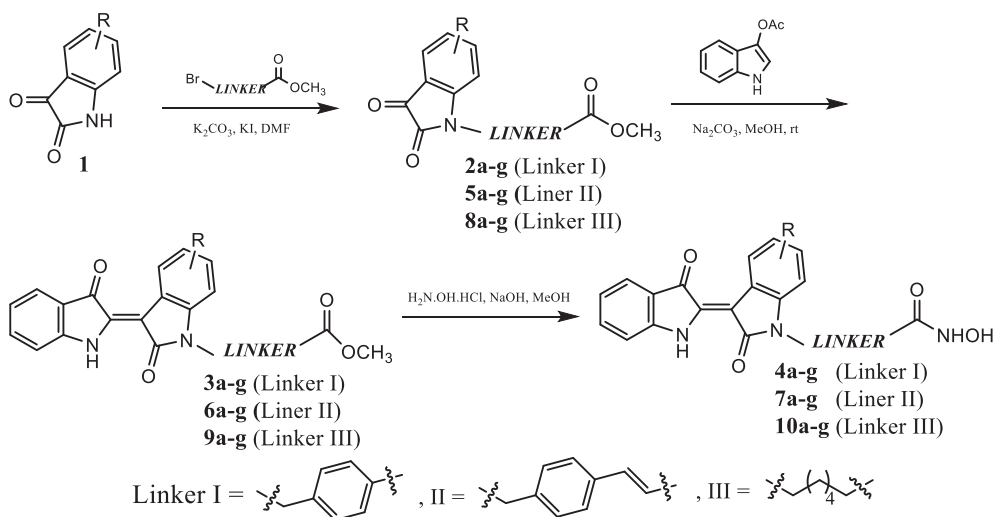
The target indirubin-based *N*-hydroxybenzamides (**4a–g**) were synthesized via a three-step pathway, as depicted in Scheme 1. Firstly, isatins (**1a–g**) reacted with methyl 4-bromobenzoate via nucleophilic substitution mechanism under basic conditions (K_2CO_3) and KI (catalytic amount) in DMF to give *N*-alkyl isatin derivatives. The yields of this step were generally from very good to excellent (85–95%). In the second step, the indirubin compounds were synthesized from the intermediates **2** and 3-indoxylacetate in presence of K_2CO_3 in DMF in good yields (~75%) were obtained. In the final step, the target hydroxamic acids were obtained by the nucleophilic acyl substitution of hydroxylamine hydrochloride with the corresponding esters **3**. This

reaction occurred under alkaline conditions, and methanol was found as an optimum solvent. Overall, compounds **4a–g** were obtained with acceptable yields under our reaction conditions (57–67%).

A series of indirubin-based *N*-hydroxypropenamides (**7a–g**) were synthesized by a similar synthetic pathway described for **4a–g**, except that methyl (*E*)-4-bromomethylcinnamate was used instead of methyl 4-bromomethylbenzoate (Scheme 1). Likewise, seven indirubin-based *N*-hydroxyheptanamides (**10a–g**) were obtained from isatin derivatives via three-step reactions (Scheme 1). The procedures were exactly the same as described for compounds **4a–g** with the modification that methyl 7-bromoheptanoate was used in place of methyl 4-bromomethylbenzoate.

Characterization of our synthesized compounds were determined straightforwardly based on analysis of IR, MS, 1H and ^{13}C NMR spectroscopic data. A singlet peak at 4.48–5.54 ppm presents two-proton for methylene moiety in the structures of **4a–g** and **7a–g**. In addition to methylene moiety, *trans*-olefinic protons were recorded as two doublets at around 6.4 and 7.4 ppm with the coupling constant (*J*) of approximately 15.5–16.0 Hz. The *2E,3Z* configuration in the indirubin skeleton has been well established.²⁵ Full NMR characterization (1H , ^{13}C) and MS can be found in Supporting Information.

The synthesized compounds were screened toward three common human cancer cell lines, including SW620, PC-3 and NCI-H23 (colon cancer, prostate cancer and lung cancer, respectively). The biological screening methodology was described previously using a colorimetric method²⁶ with slight modifications.^{27–29} The IC_{50} values were calculated as averages from three independent experiments using a Probits method³⁰. SAHA and adriamycin (ADR) were used as a positive control. The overall screening results were summarized in Table 1. Generally, our synthesized compounds exhibited very potent cytotoxicity against all three human cancer cell lines tested with IC_{50} values of 0.09 μM or lower as shown in Table 1. Seven compounds, including **4e**, **7a–c**, **7e**, **10b**, and **10e**, even showed IC_{50} values lower than 0.01 μM in NCI-H23 cell line. The IC_{50} values of adriamycin, a strongly cytotoxic anticancer drug currently used widely in clinical setting, were 0.09 μM



Scheme 1. Synthesis of indirubin-based *N*-hydroxybenzamides (4a-g), *N*-hydroxypropenamides (7a-g), and *N*-hydroxyheptanamides (10a-g); a, R = H; b, R = 5-F; c, R = 5-Cl; d, R = 7-Cl; e, R = 5-Br; f, R = 5-CH₃; g, R = 5-OCH₃.

Table 1

Inhibition of HDAC activity in Hela cell extract and cytotoxicity of the synthesized compounds against several human cancer cell lines.

Cpd. code	R	HDAC (Hela extract) Inhibition (IC ₅₀ , ¹ μM)	Cytotoxicity (IC ₅₀ , ¹ μM)/Cell lines ²		
			SW620	PC3	NCI-H23
4a	H	0.195 ± 0.041	0.07 ± 0.03	0.06 ± 0.02	0.07 ± 0.03
4b	5-F	0.218 ± 0.019	0.02 ± 0.01	0.05 ± 0.001	0.03 ± 0.001
4c	5-Cl	0.174 ± 0.022	0.06 ± 0.03	0.05 ± 0.001	0.05 ± 0.001
4d	7-Cl	0.071 ± 0.001	0.09 ± 0.001	0.06 ± 0.001	0.06 ± 0.001
4e	5-Br	0.039 ± 0.004	0.07 ± 0.02	0.05 ± 0.01	0.007 ± 0.000
4f	5-CH ₃	0.005 ± 0.001	0.03 ± 0.001	0.09 ± 0.001	0.01 ± 0.001
4g	5-OCH ₃	0.025 ± 0.003	0.04 ± 0.01	0.03 ± 0.01	0.09 ± 0.001
7a	H	0.095 ± 0.024	0.05 ± 0.01	0.05 ± 0.001	0.009 ± 0.002
7b	5-F	0.422 ± 0.074	0.05 ± 0.01	0.05 ± 0.001	0.008 ± 0.001
7c	5-Cl	0.318 ± 0.064	0.08 ± 0.01	0.06 ± 0.04	0.007 ± 0.001
7d	7-Cl	0.604 ± 0.050	0.06 ± 0.01	0.09 ± 0.01	0.05 ± 0.01
7e	5-Br	0.183 ± 0.003	0.06 ± 0.01	0.09 ± 0.001	0.009 ± 0.001
7f	5-CH ₃	0.020 ± 0.008	0.05 ± 0.01	0.06 ± 0.01	0.01 ± 0.001
7g	5-OCH ₃	0.005 ± 0.000	0.04 ± 0.001	0.03 ± 0.001	0.05 ± 0.01
10a	H	0.022 ± 0.000	0.09 ± 0.001	0.05 ± 0.02	0.09 ± 0.001
10b	5-F	0.014 ± 0.006	0.08 ± 0.01	0.012 ± 0.001	0.008 ± 0.001
10c	5-Cl	0.003 ± 0.000	0.06 ± 0.02	0.09 ± 0.001	0.03 ± 0.01
10d	7-Cl	0.007 ± 0.000	0.09 ± 0.001	0.03 ± 0.001	0.05 ± 0.01
10e	5-Br	0.004 ± 0.000	0.09 ± 0.001	0.03 ± 0.001	0.009 ± 0.001
10f	5-CH ₃	0.018 ± 0.005	0.05 ± 0.001	0.08 ± 0.02	0.010 ± 0.001
10g	5-OCH ₃	0.021 ± 0.001	0.03 ± 0.01	0.05 ± 0.01	0.07 ± 0.02
Indirubin-3'-oxime	#	13.5 ± 2.18	15.8 ± 2.81	11.25 ± 2.11	
SAHA ³	0.025 ± 0.002	1.12 ± 0.10	1.82 ± 0.09	1.44 ± 0.17	
ADR ⁴	#	0.09 ± 0.001	0.09 ± 0.001	0.09 ± 0.001	

¹ The concentration (μM) of compounds that produces a 50% reduction in enzyme activity or cell growth, the numbers represent the averaged results from triplicate experiments; ²Cell lines: SW620, colon cancer; PC3, prostate cancer; NCI-H23, lung cancer; ³SAHA, suberoylanilide acid, a positive control; ⁴ADR, adriamycin, a positive control.

in all three cancer cell lines. Thus, in term of cytotoxicity, it was clear that all compounds from three series 4a-g, 7a-g and 10a-g were equipotent or even more potent than adriamycin towards these human cancer cell lines. Against SW620 cells, the compounds (IC₅₀ values of 0.09–0.02 μM) were found to be approximately 12-fold to 56-fold more potent than SAHA (IC₅₀ value of 1.12 μM). Against PC3 cells, the compounds (IC₅₀ values of 0.012–0.09 μM) were found to be from 20- to approximately 152-fold as potent as SAHA (IC₅₀ value of 1.82 μM).

Meanwhile, against NCI-H23 cells the compounds (IC₅₀ values of 0.007–0.09 μM) were found to be about 15-fold to 205-fold as potent as SAHA (IC₅₀ value of 1.44 μM). The IC₅₀ values for indirubin-3'-oxime against SW620, PC-3 and NCI-H23 cell lines were 13.5 ± 2.18, 15.8 ± 2.81, and 11.25 ± 2.11 μM, respectively. Other 5-/7-substitutedindirubin-3'-oxime derivatives all showed weak cytotoxicity in the above three cancer cell lines with IC₅₀ values of > 10 μM (data not shown). These results clearly demonstrate that hybridization of the

Table 2
Inhibition of HDAC2 and HDAC6 isoforms by compounds **4a-g**.

Cpd. code	R	HDAC2 inhibition (IC ₅₀ , ¹ μM)	HDAC6 inhibition (IC ₅₀ , ¹ μM)	Cpd. Code	R	HDAC2 inhibition (IC ₅₀ , ¹ μM)	HDAC6 inhibition (IC ₅₀ , ¹ μM)
4a	H	0.205 ± 0.038	0.007 ± 0.001	4e	5-Br	0.075 ± 0.006	0.024 ± 0.001
4b	5-F	0.194 ± 0.017	0.043 ± 0.001	4f	5-CH ₃	0.021 ± 0.002	0.020 ± 0.002
4c	5-Cl	0.187 ± 0.015	0.016 ± 0.000	4g	5-OCH ₃	0.031 ± 0.005	0.030 ± 0.002
4d	7-Cl	0.088 ± 0.001	0.049 ± 0.000	SAHA ²		0.033 ± 0.003	0.030 ± 0.001

¹ The concentration (μM) of compounds that produces a 50% reduction in enzyme activity. ²SAHA, suberoylanilide acid, a positive control.

Table 3
Binding energies estimated for all compounds docked into HDAC2 and HDAC6 enzymes.

Cpd. code	HDAC2				HDAC6			
	E_Score1**	E_score2**	Distance to Zn ²⁺ *		E_Score1	E_score2	Distance to Zn ²⁺	
			–OH	=O			–OH	=O
4a	–19.822	–7.578	2.19	2.35	–22.762	–11.598	2.09	2.06
4b	–17.371	–6.246	2.35	2.39	–18.542	–10.110	2.13	2.10
4c	–20.137	–7.367	2.35	2.19	–21.569	–11.121	2.07	2.06
4d	–20.772	–6.918	2.18	2.20	–16.393	–10.502	2.09	2.07
4e	–20.238	–9.065	2.16	2.30	–18.421	–10.796	2.08	2.05
4f	–23.119	–9.676	2.18	2.23	–20.142	–10.523	2.19	2.03
4g	–21.747	–8.725	2.16	2.32	–18.497	–10.987	2.08	2.03
SAHA	–20.884	–8.287	2.18	2.29	–20.231	–10.664	2.07	2.07
TSA					–17.547	–11.064	2.13	1.96

* The docking score (kcal/mol) calculated from the London (with refinement) and affinity scoring function from MOE software.

** Distances (Å) from oxygen atoms (–O and =O) of hydroxamate group to zinc ion.

indirubin-3'-oxime or 5-/7-substituted-indirubin-3'-oxime derivatives with *N*-hydroxybenzamide, *N*-hydroxypropenamide or *N*-hydroxyheptannamide scaffolds has strongly enhanced the cytotoxicity of the indirubin-3'-oximes and furnished powerful cytotoxic agents. All compounds in three series **4a-g**, **7a-g** and **10a-g** have logP values in the range of 2.20–3.17, as calculated by KowWin program v1.67, thus favorable and promising for further development as orally active anticancer agents.

The addition of the hydroxamic acid scaffolds to the indirubin-3'-oxime cores resulted in compounds **4a-g**, **7a-g** and **10a-g** with cytotoxicity thousand-fold more potent than the original indirubin-3'-oximes. Thus, compounds **4a-g**, **7a-g** and **10a-g** would be expected to act more prominently as HDAC inhibitors. We therefore evaluated the compounds for their inhibition of HDAC using a Fluorogenic HDAC Assay Kit (abcam, MA, USA) with SAHA as a positive control. The results of inhibition of HDAC are also presented in Table 1. As the results demonstrate, all compounds in three series **4a-g**, **7a-g** and **10a-g** were potent HDAC inhibitors with IC₅₀ values ranging from 0.003 to 0.604 μM. Within the *N*-hydroxybenzamides **4a-g**, compound **4b** with 5-fluoro substituent (IC₅₀, 0.218 μM) was slightly less potent than the unsubstituted one (**4a**, IC₅₀, 0.195 μM). All other compounds in the series were more potent than **4a**. Chloro substituted at position 7 (**4d**, IC₅₀, 0.071 μM) seemed to better enhanced the HDAC inhibition than 5-chlorosubstitution (**4c**, IC₅₀, 0.174 μM). Bulkier halogen (e.g. Br) and electron-releasing substituents (–CH₃, –OCH₃) were more favorable for HDAC inhibition ((**4e-g**, IC₅₀, 0.039, 0.005, and 0.025 μM, respectively). For *N*-hydroxypropenamides (**7a-g**), a very clear structure-activity relationship was observed. Electron-withdrawing substituents (–F, –Cl, and –Br) reduced the HDAC inhibition, while electron-releasing substituents (–CH₃, –OCH₃) significantly enhanced the HDAC inhibitory activity of the compounds. In this series, it seemed that bulkier substituents (–Br, –OCH₃) were more favorable for bioactivity. It was interesting to note that compounds **4f**, **4g** and compounds **7f**, **7g** bearing 5-CH₃ and 5-OCH₃ substituents were the most potent HDAC inhibitors among the compounds in two series **4a-g** and **7a-g**.

Seven compounds in series **10a-g** were the most potent HDAC inhibitors among three series with IC₅₀ values from 0.003 to 0.022 μM).

In this series, both electron-withdrawing substituents (–F, –Cl, –Br) or electron releasing substituents were favorable for HDAC inhibition. Considering in more detail, it could be noted that, the electron-withdrawing substituents (–F, –Cl, –Br) more strongly enhanced the HDAC inhibitory activity, as manifested by the IC₅₀ values of compounds **10b-e** (0.003–0.014 μM) vs. compounds **10f, g** (0.018–0.025 μM). All compounds in series **10a-g** were more potent than SAHA in term of HDAC inhibition, which correlated well with their stronger cytotoxicity in comparison to SAHA. However, in series **7a-g**, and also in series **4a-g**, some compounds were less potent as HDAC inhibitors in comparison to SAHA, but exhibited much stronger cytotoxicity than SAHA in all three human cancer cell lines assayed. It is likely that these compounds might act on other targets of the indirubin-3'-oxime cores (e.g. cyclin-dependent kinases, CDKs) and this possibility remains to be investigated further. On the other hand, compounds bearing *N*-hydroxybenzamide scaffolds have recently been demonstrated as more selective inhibitors of HDAC6 isoform.³¹ Meanwhile, a Fluorogenic HDAC Assay Kit using an HDAC extract which is a rich source of HDAC activity, but contains predominantly class-I isoforms (HDAC1, 2, 3, and 8).³² Considering this information, it is possible that the current *N*-hydroxybenzamides **4a-g** might possess better inhibitory effects against HDAC6 isoform. We therefore decided to evaluate compounds **4a-g** for their inhibitory effects against HDAC6 isoform. HDAC2, a representative of Class-I HDACs was included. The results are summarized in Table 2. It is very interesting to note that 5 compounds, including **4a-e**, showed more potent inhibitory activity against HDAC6, as compared to HDAC2. Especially, compound **4a** inhibited HDAC6 with an IC₅₀ value of 0.007 μM, 29-fold lower than its IC₅₀ value against HDAC2 isoform (0.205 μM). Compounds **4b** and **4c** exhibited 4.5- and 11.7-fold more potent inhibition towards HDAC6 in comparison to HDAC2 (IC₅₀ values of 0.043 and 0.016 μM vs. 0.194 and 0.187 μM, respectively). Thus, from this study, compound **4a** showed potentials as a lead compound for further development of HDAC6 potent inhibitors in the future.

In addition to cytotoxicity and HDAC inhibition, three representative compounds, including **4a**, **7a** and **10a**, were selected to investigate for their effects on cell cycle and apoptosis using flow

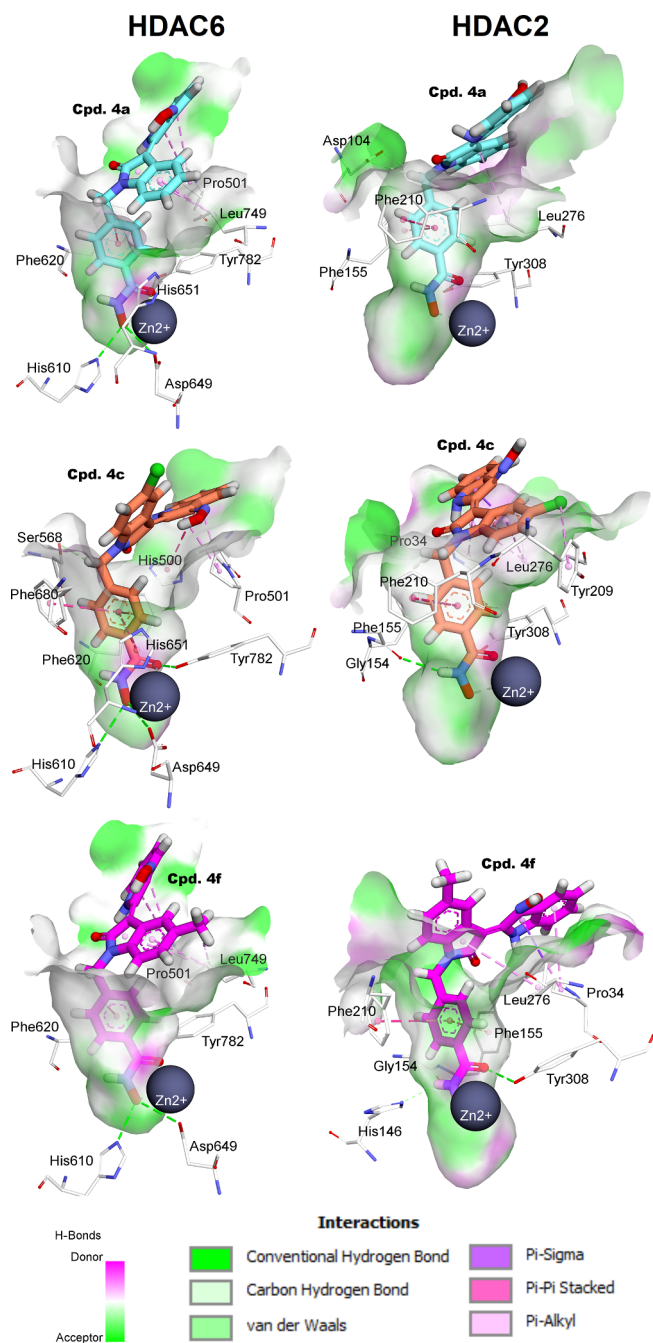


Fig. 2. Docking poses of compounds **4a**, **4c** and **4f** inside the active site of HDAC2 and HDAC6.

cytometry technique. It was found that compounds **7a** and **10a** significantly induced early apoptosis of SW620 cells at a level similar to that observed with SAHA. Compound **4a** appeared to significantly arrest cells at G0/G1 phase meanwhile compound **7a** was found to significantly arrest cells at both G0/G1 and S phases (See Figs. S1–S5, Supporting Information).

Based on the experimental evaluations, a comparative docking study was performed for compounds of series **4a–g** against HDAC6 and HDAC2 (PDB ID: 4LXZ and 5EDU, respectively), a preferentially expressed Class-I isoform in Hela nuclear extract,³³ in order to figure out which chemical features could be responsible for HDAC selectivity. To validate the docking procedures applied, redocking simulations were performed with the native ligands. As the results, after redocking in the binding site of HDAC6, TSA was highly overlapped with the co-crystal

ligand (the RMSD value of 0.563 Å). The main interactions between TSA and residues in the active site of HDAC6 were conserved, including H-bonds with His610, His651 and Tyr782, and stacking interactions with Pro501, Phe620 and Phe680. On the other hands, SAHA was redocked into the active sites of HDAC2 and HDAC6 enzymes. As the results, the redocked and co-crystal poses of SAHA in HDAC2 were appropriately superimposed (RMSD of 0.823 Å). All the key interactions with Asp104, His145, and Tyr308 (H-bonds), His33 and Pro34 (hydrophobic interactions) were conserved. In addition, the docking results of SAHA against HDAC6 highlighted the importance of multiple H-bonding interactions with residues at the base of the pocket, especially His610, His611, His651 and Tyr782 (Fig. S6). These results were consistent with those reported previously.³⁴

After validating the docking method, all the compounds **4a–g** were docked into HDAC2 and HDAC6 isoforms. In general, these compounds were well accommodated in the pockets of the two enzymes. The free binding energies dG were computed after energy minimization using the London (E_{score1}) and affinity GBVI/WSA (E_{score2}) scoring functions.²¹ Interestingly these functions matched well with the experimental assessments. As can be seen in Table 3, **4f** exhibited the highest energy with HDAC2, meanwhile **4a** and **4c** showed the best scores in complex with HDAC6; all of them showed higher dG values than reference compounds SAHA and TSA. On the basis of *in vitro* tests in HDAC6, the correlation between $\log(E_{\text{score1}})$ and IC_{50} (R^2) was $\sim 80\%$, higher than that of function between E_{score2} and $\log IC_{50}$ ($R_2 \sim 73\%$), suggesting a suitable rank-order relationship between experimental and computational estimations.

As can be seen in Fig. 2, **4a** exhibited similar interactions to TSA in the HDAC6 pocket. However, **4a** docked into HDAC2 did not show H-bond interactions with the key residues at the base of the pocket, such as His145, His146, Asp181, His183 and Asp269. On the other hands, oxindoline with 5-halogen substituents lacked of double stacking interactions with Leu749 while forming two additional van der Waals interactions with Ser568. Enhancement of the hydrophobic interactions with residues at the entrance of the pocket, including His500, Pro501 and Ser568 from **4b** to **4e** could be observed. These interactions could make positive effect on selectivity towards HDAC6 but this effect decreases from fluorine to bromine analogues (**4b**, **4c**, **4e**). In contrast to **4a**, **4f** showed better interactions with HDAC2 compared to HDAC6. This compound regenerated a complex H-bonding network from the hydroxamate group towards residues His146, Gly154 and Tyr308 of HDAC2. At last, the indirubin capping groups showed multiple pi stacking interactions with hydrophobic residues at the entrance of HDAC pockets, such as Pro34, Leu276 (HDAC2), and Pro501, Leu740 (HDAC6). Given the importance of bulky branched cap groups for improving protein surface interaction as well as HDAC isoform-selectivity (e.g. HDAC6),³⁵ it is emphasized the roles of indirubins as promising capping groups in designing potent, selective HDAC inhibitors.

More than 40% potential therapeutic agents fail to be an effective clinical candidate because of their unfavorable absorption, distribution, metabolism, elimination and toxic (ADMET) factors.³⁶ We therefore evaluated accomplishment of Lipinski's Ro5. The results (shown in Table S1, Supporting Information) demonstrate that these compounds fulfilled Ro5 criteria and possessed satisfactory ADMET profile. In comparison to SAHA (ZolinzaTM), compounds **4f** and **7g** show favorable physicochemical and pharmacokinetic profiles similar to the reference compound. In our opinion, these results served as a good starting point for further structural optimization for new anticancer agents.

In conclusion, we have reported three series of indirubin-based *N*-hydroxybenzamides, *N*-hydroxypropenamides, and *N*-hydroxyheptanamides with excellent HDAC inhibitory activities and potent cytotoxicity towards three human cancer cell lines, including SW620, PC-3 and NCI-H23 (colon cancer, prostate cancer and lung cancer, respectively). Most compounds displayed cytotoxicity of 20- to more than 205-fold stronger than SAHA. In term of cytotoxicity our synthesized compounds were also equipotent or even more potent than that of

adriamycin against three human cancer cell lines tested. These compounds also inhibited HDACs comparably or more potently than SAHA with IC₅₀ values as low as 0.003 μM. The *N*-hydroxyheptanamides (**10a-g**) were found to be the most potent with strong HDAC inhibition and excellent cytotoxicity. The results we obtained from this study again confirm that the indirubin-3'-oxime could well serve as a cap group for HDAC inhibitors. Also, the hybridization between the indirubin-3'-oxime and hydroxamic acid greatly enhanced both HDAC inhibition and cytotoxicity of the resulting compounds. Docking studies revealed some features (e.g. bulkier and shorter aromatic linker, 5-halogen substitutions) could enhance the selectivity towards HDAC6 isoform compared to class I HDAC enzymes. In addition, our ADMET predictions indicated that several compounds, including **4f** and **7g** could be potential candidates for further drug development.

Declaration of Competing Interest

The authors declare that they have no known competing financial interests or personal relationships that could have appeared to influence the work reported in this paper.

Acknowledgements

We acknowledge the principal financial supports from the National Foundation for Science and Technology of Vietnam (NAFOSTED, Grant number 104.01-2019.09). The work was also partly supported by a grant funded by the Korean Government (NRF-2017R1A5A2015541).

Appendix A. Supplementary data

Supplementary data to this article can be found online at <https://doi.org/10.1016/j.bmcl.2020.127537>.

References

- Hamm CA, Costa FF. Epigenomes as therapeutic targets. *Pharmacol Ther*. 2015;151:72–86.
- Ruijter AJM, Gennip AH, Caron HN, Kemp S, Kuilenburg ABP. Histone deacetylases (HDACs): characterization of the classical HDAC family. *Biochem J*. 2003;370(3):737–749.
- Witt O, Deubzer HE, Milde T, Oehme I. HDAC family: what are the cancer relevant targets? *Cancer Lett*. 2009;277(1):8–21.
- Ververis K, Hiong A, Karagiannis TC, Licciardi PV. Histone deacetylase inhibitors (HDACIs): multitargeted anticancer agents. *Biologics*. 2012;7:47–60.
- Valente S, Mai A. Small-molecule inhibitors of histone deacetylase for the treatment of cancer and non-cancer diseases: a patent review (2011–2013). *Expert Opin Ther Pat*. 2014;24(4):401–415.
- Jiyang L, Guangqiang L, Wenqing X. Histone deacetylase inhibitors: an attractive strategy for cancer therapy. *Curr Med Chem*. 2013;20(14):1858–1886.
- Zwergel C, Valente S, Jacob C, Mai A. Emerging approaches for histone deacetylase inhibitor drug discovery. *Expert Opin Drug Discov*. 2015;10(6):599–613.
- West AC, Johnstone RW. New and emerging HDAC inhibitors for cancer treatment. *J Clin Invest*. 2014;124(1):30–39.
- Bolden JE, Peart MJ, Johnstone RW. Anticancer activities of histone deacetylase inhibitors. *Nat Rev Drug Discov*. 2006;5(9):769–784.
- Iyer SP, Foss FF. Romidepsin for the treatment of peripheral T-Cell lymphoma. *Oncologist*. 2015;20(9):1084–1091.
- Guha M. HDAC inhibitors still need a home run, despite recent approval. *Nat Rev Drug Discov*. 2015;14(4):225–226.
- Qiu T, Zhou L, Zhu W, et al. Effects of treatment with histone deacetylase inhibitors in solid tumors: a review based on 30 clinical trials. *Future Oncol*. 2013;9(2):255–269.
- Bracker TU, Sommer A, Fichtner I, Faus H, Haendler B, Hess-Stumpff H. Efficacy of MS-275, a selective inhibitor of class I histone deacetylases, in human colon cancer models. *Int J Oncol*. 2009;35(4):909–920.
- Glaser KB. HDAC inhibitors: Clinical update and mechanism-based potential. *Biochem Pharmacol*. 2007;74(5):659–671.
- Oanh DTK, Hai HV, Park SH, et al. Benzothiazole-containing hydroxamic acids as histone deacetylase inhibitors and antitumor agents. *Bioorg Med Chem Lett*. 2011;21(24):7509–7512.
- Nam N-H, Huong TL, Dung DTM, et al. Synthesis, bioevaluation and docking study of 5-substitutedphenyl-1,3,4-thiadiazole-based hydroxamic acids as histone deacetylase inhibitors and antitumor agents. *J Enzyme Inhib Med Chem*. 2014;29(5):611–618.
- Nam N-H, Huong TL, Mai Dung DT, et al. Novel isatin-based hydroxamic acids as histone deacetylase inhibitors and antitumor agents. *Eur J Med Chem*. 2013;70:477–486.
- Huong TTL, Dung DTM, Dung PTP, et al. Novel 2-oxindoline-based hydroxamic acids: synthesis, cytotoxicity, and inhibition of histone deacetylation. *Tetrahedron Lett*. 2015;56(46):6425–6429.
- Huong TTL, Van Cuong L, Huong PT, et al. Exploration of some indole-based hydroxamic acids as histone deacetylase inhibitors and antitumor agents. *Chem Pap*. 2017;71(9):1759–1769.
- Do TMD, Phan TPD, Dao TKO, et al. Novel 3-substituted-2-oxindoline-based *N*-hydroxypropenamides as histone deacetylase inhibitors and antitumor agents. *Med Chem*. 2015;11(8):725–735.
- Hieu DT, Anh DT, Tuan NM, et al. Design, synthesis and evaluation of novel *N*-hydroxybenzamidic/*N*-hydroxypropenamides incorporating quinoxalin-4(3H)-ones as histone deacetylase inhibitors and antitumor agents. *Bioorg Chem*. 2018;76:258–267.
- Huong T-T-L, Dung D-T-M, Huan N-V, et al. Novel *N*-hydroxybenzamidic incorporating 2-oxindoline with unexpected potent histone deacetylase inhibitory effects and antitumor cytotoxicity. *Bioorg Chem*. 2017;71:160–169.
- Truong Thanh T, Dao Thi Kim O, Phan Thi Phuong D, et al. New benzothiazole/thiazole-containing hydroxamic acids as potent histone deacetylase inhibitors and antitumor agents. *Med Chem*. 2013;9(8):1051–1057.
- Cheng X, Merz K-H. The role of indirubins in inflammation and associated tumorigenesis. In: Gupta SC, Prasad S, Aggarwal BB, eds. *Drug Discovery from Mother Nature*. Cham: Springer International Publishing; 2016:269–290.
- Lin W-J, Shia K-S, Song J-S, Wu M-H, Li W-T. Synthesis of (E)-oxindolylidene acetate using tandem palladium-catalyzed Heck and alkoxycarbonylation reactions. *Org Biomol Chem*. 2016;14(1):220–228.
- Skehan P, Storeng R, Scudiero D, et al. New colorimetric cytotoxicity assay for anticancer-drug screening. *JNCI: J Natl Cancer Inst*. 1990;82(13):1107–1112.
- Nam N-H, Pitts RL, Sun G, et al. Design of tetrapeptide ligands as inhibitors of the Src SH2 domain. *Bioorg Med Chem*. 2004;12(4):779–787.
- Nam NH, Hong DH, You YJ, et al. Synthesis and cytotoxicity of 2,5-dihydroxy-chalcones and related compounds. *Arch Pharm Res*. 2004;27(6):581–588.
- Min B-S, Huong H-T-T, Kim J-H, et al. Furo-1,2-naphthoquinones from *Crataegus pinnatifida* with ICAM-1 Expression Inhibition Activity. *Planta Med*. 2004;70(12):1166–1169.
- Wu L, Smythe AM, Stinson SF, et al. Multidrug-resistant phenotype of disease-oriented panels of human tumor cell lines used for anticancer drug screening. *Cancer Res*. 1992;52(11):3029.
- Blackburn C, Barrett C, Chin J, et al. Potent histone deacetylase inhibitors derived from 4-(Aminomethyl)-*N*-hydroxybenzamide with high selectivity for the HDAC6 isoform. *J Med Chem*. 2013;56(18):7201–7211.
- Pelzel HR, Schlamp CL, Nickells RW. Histone H4 deacetylation plays a critical role in early gene silencing during neuronal apoptosis. *BMC Neurosci*. 2010;11(1):62.
- Weichert W, Röske A, Gekeler V, et al. Histone deacetylases 1, 2 and 3 are highly expressed in prostate cancer and HDAC2 expression is associated with shorter PSA relapse time after radical prostatectomy. *Br J Cancer*. 2008;98(3):604–610.
- Do TMD, Nguyen VH, Do MC, et al. Novel hydroxamic acids incorporating 1-((1H-1,2,3-Triazol-4-yl)methyl)-3-substituted-2-oxindolines: synthesis, biological evaluation and SAR analysis. *Med Chem*. 2018;14(8):831–850.
- Yang F, Zhao N, Ge D, Chen Y. Next-generation of selective histone deacetylase inhibitors. *RSC Adv*. 2019;9(34):19571–19583.
- van de Waterbeemd H, Gifford E. ADMET in silico modelling: towards prediction paradise? *Nat Rev Drug Discov*. 2003;2(3):192–204.